Bone 124 (2019) 137–147

Contents lists available at ScienceDirect

Bone

journal homepage: www.elsevier.com/locate/bone

Full Length Article

Sclerostin antibody reduces long bone fractures in the oim/oim model of osteogenesis imperfecta

Mickaël Cardinal[a,*], Janne Tys[a], Thomas Roels[a], Sébastien Lafont[a], Michael S. Ominsky[c], Jean-Pierre Devogelaer[b], Daniel Chappard[d], Guillaume Mabilleau[d], Patrick Ammann[e], Catherine Nyssen-Behets[a], Daniel H. Manicourt[b]

[a] Pole of Morphology, Institut de Recherche Expérimentale et Clinique, UCLouvain, Brussels, Belgium
[b] Pole of Rheumatic Pathologies, Institut de Recherche Expérimentale et Clinique, UCLouvain, Brussels, Belgium
[c] Radius, Inc., Waltham, MA, USA, formerly at Amgen Inc, Thousand Oaks, CA, USA
[d] GEROM-LHEA and SCIAM, University of Angers, France
[e] Division of Bone Diseases, Department of Internal Medicine Specialties, Geneva University Hospital, Geneva, Switzerland

ARTICLE INFO

Keywords:
Osteogenesis imperfecta
Oim/Oim
Sclerostin antibody
Fracture
Biomechanical strength
Bone quality

ABSTRACT

Osteogenesis imperfecta type III (OI) is a serious genetic condition with poor bone quality and a high fracture rate in children. In a previous study, it was shown that a monoclonal antibody neutralizing sclerostin (Scl-Ab) increases strength and vertebral bone mass while reducing the number of axial fractures in oim/oim, a mouse model of OI type III. Here, we analyze the impact of Scl-Ab on long bones in OI mice. After 9 weeks of treatment, Scl-Ab significantly reduced long bone fractures (3.6 ± 0.3 versus 2.1 ± 0.8 per mouse, $p < 0.001$). In addition, the cortical thickness of the tibial midshaft was increased (+42%, $p < 0.001$), as well as BMD (+28%, $p < 0.001$), ultimate load (+86%, $p < 0.05$), plastic energy (+184%; $p < 0.05$) and stiffness (+172%; $p < 0.01$) in OI Scl-Ab mice compared to OI vehicle controls. Similar effects of Scl-Ab were observed in Wild type (Wt) mice. The plastic energy, which reflects the fragility of the tissue, was lower in the OI than in the Wt and significantly improved with the Scl-Ab treatment. At the tissue level by nanoindentation, Scl-Ab slightly increased the elastic modulus in bones of both OI and Wt, while moderately increasing tissue hardness (+13% compared to the vehicle; $p < 0.05$) in Wt bones, but not in OI bones. Although it did not change the properties of the OI bone matrix material, Scl-Ab reduced the fracture rate of the long bones by improving its bone mass, density, geometry, and biomechanical strength. These results suggest that Scl-Ab can reduce long-bone fractures in patients with OI.

1. Introduction

Osteogenesis imperfecta (OI) is the prototype of severe osteoporosis with recurrent bone fractures throughout life. OI is the most frequent bone dysplasia (8/100,000 live births) and has no cure [1]. The disease results from mutations in the quantity and quality of type I collagen. Its variable phenotype depends on the type and position of the causal mutation [2–4]. Almost all patients suffer fractures of the extremities long bones that are produced by minimal trauma [5]. In severe disease, children suffer dozens of fractures and multiple deformity of long bones before reaching adolescence. Even in mild disease, the risk of long bone fracture is 95 times higher than in a healthy population [6]. The rate of fractures decreases after puberty but may increase again in women after menopause [7]. In addition to skeletal deformations, patients with OI also present variable combinations of growth deficiency, hearing loss, defective teeth formation and blue sclera.

Because the wide clinical range of OI interferes with the prognosis of the disease and therapeutic interventions, patients are classified into five phenotypes [4]. Among them, type III is the most severe form compatible with life. Neonates with type III OI already have multiple

* Corresponding author at: Pole of Morphology, Institut de Recherche Expérimentale et Clinique, UCLouvain, 52 Avenue Mounier - B1.52.04, B-1200 Brussels, Belgium.
E-mail addresses: mickael.cardinal@uclouvain.be (M. Cardinal), janne.tys@uclouvain.be (J. Tys), thomas.roels@uclouvain.be (T. Roels), sebastien.lafont@uclouvain.be (S. Lafont), ominsky@umich.edu (M.S. Ominsky), jean-pierre.devogelaer@uclouvain.be (J.-P. Devogelaer), daniel.chappard@univ-angers.fr (D. Chappard), guillaume.mabilleau@univ-angers.fr (G. Mabilleau), Patrick.Ammann@hcuge.ch (P. Ammann), catherine.behets@uclouvain.be (C. Nyssen-Behets), daniel.manicourt@uclouvain.be (D.H. Manicourt).

https://doi.org/10.1016/j.bone.2019.04.011
Received 25 December 2018; Received in revised form 31 March 2019; Accepted 22 April 2019
Available online 30 April 2019

fractures. Low bone mass, changes in bone morphology and alterations in the bone matrix contribute to the severity of bone fragility and subsequent skeletal deformations [3,8,9].

Bone fragility contributes greatly to severe disability in OI [10,11]. Many type III patients never walk independently, regardless of their treatment [5]. In addition to missed school days, pain and disability, immobilization related to fractures worsens the patient's osteopenia. Surgical correction of deformation with intramedullary rod may help ambulation [12,13], but OI long bones stabilized with bars remain soft and continue to break, especially at the tips of the bars and at sites of rupture or osteotomy [14]. Therefore, medical treatments must imperatively increase the strength of the OI bones.

Since the strength of a bone is related to its quantity, the increase in bone mass should, in theory, strengthen OI bones, despite its abnormal collagen matrix. Because antiresorptive drugs prevent bone loss, many doctors prescribe bisphosphonates (BP) to children with OI for 2 to 5 years with justification to maximize their impact on a growing skeleton. In controlled trials, BP improved vertebral bone density and geometry in children with type III and IV OI (average age: 3 to 16 years) [15] but failed to reduce long bone fractures, more particularly in the lower extremity [16–19]. In addition, the long-term accumulation of BP in the bone matrix and the associated inhibition of bone remodeling could further affect the bone quality by a high degree of bone mineralization, as described in human [20–23] and murine studies [24,25].

As the activity of osteoblastic cells decreases in OI [26], the anabolic properties of anti–sclerostin antibody (Scl-Ab) were investigated. Sclerostin (Scl) is a glycoprotein encoded by the SOST gene and produced by the osteocyte. It is a potent antagonist of the canonical Wnt signaling pathway in osteoblasts and, therefore, a negative regulator of bone formation [27,28]. In fact, the loss of function of the SOST gene causes a phenotype of high bone mass and improves bone strength [29]. In addition, the pharmacological inhibition of sclerostin by monoclonal Scl-Ab has a marked bone-forming effect in both healthy men and postmenopausal women, as well as in several animal models of osteoporosis [30,31].

To date, treatment with Scl-Ab has been evaluated in two mouse models of moderate OI (Brtl/+ and col1a2$^{+/p.G610C}$) and two mouse models of severe OI (Col1a1^{jrt}/+ and Crtap−/−). Scl-Ab improved bone mass and strength in all of them [32–37]. Surprisingly, these studies did not provide any information on the number of fractures in mice treated with placebo and Scl-Ab.

The primary objective of the treatment of children and adolescents with OI is to reduce the fragility of the skeleton, more particularly in the appendicular bones where the majority of fractures occur [38]. Therefore, we tested the effect of Scl-Ab in oim/oim mice, a well-established mouse model of severe type III OI. Indeed, oim/oim mice have frequent fractures, small size, osteopenia and bone deformities [39,40]. We treated young female wildtype (Wt) and oim/oim mice with Scl-Ab for 9 weeks and focused mainly on the fracture rate and structural properties of long bones.

2. Materials and methods

2.1. Animals

We used homozygous oim/oim mice (B6C3Fe strain a/a-Col1a2oim/J), homozygous wildtype mice (strain B6C3Fe-a/a+/+, SN1815) and B6C3 mice for the OI mutation (Charles River Laboratories, 69592 L'Arbresle, France). We performed weaning at 4 weeks. The genotype of the mice was monitored by PCR amplifying the purified genomic DNA from tail cut samples [41], using the primers (1) ggctttcctagaccccgatgcttag as forward; (2) gtcttgccccattcatttgtc as Wt reverse; and (3) gtcttgccccattcatttgtt as OI reverse.

All procedures with animals are in accordance with the Belgian federal law for the care of animals. The ethics committee for animal research of the Université Catholique de Louvain approved the protocols, handling and care of mice. We fed and housed mice under standard rodent conditions. As OI mice show marked bone fragility, they were sedated to facilitate smooth handling. We injected ketamine for radiographs and used sevoflurane inhalation to facilitate other procedures, such as subcutaneous injections [42]. The mice were euthanized by sevoflurane inhalation.

2.2. Treatment

Five-week-old female wildtype (Wt) and oim/oim (OI) mice were randomly assigned to an anti-sclerostin antibody (Scl-Ab) dissolved in the PBS vehicle (Amgen Inc., Thousand Oaks, CA, USA) or to a vehicle injection of PBS (Veh.). Scl-Ab was injected subcutaneously at 50 mg/kg once a week for 9 weeks. In order to facilitate dynamic histomorphometry, calcein (10 mg/kg) was injected intraperitoneally on experimental days 1, 21, 42 and 63, just before euthanasia.

2.3. Fracture count

High-resolution anteroposterior and mediolateral radiographs were obtained using a mammography system. In OI Veh. and OI Scl groups, 10 mice were radiographed the first and fourth week of treatment to provide a baseline fracture number. We had to add mice in OI groups to compensate their relatively higher mortality. After euthanasia at the end of the study, all the mice of both OI groups (n = 15 per groups) were X-rayed. Two independent observers blinded to the group assignment counted fractures in the femurs, tibias, humerus, and forearms. We defined the fractures by evidence of solution of continuity, callus formation, and patent bone deformity.

Thereafter, all tests were performed on intact dissected bones, excluding the fractured ones. We then assigned the available intact bones to the various procedures, which explains their different “n” values.

2.4. Bone geometry

After dissecting and cleaning the humerus and tibias, we evaluated the external volume of the tibias according to the Archimedes' principle with a Density Accessories kit (Mettler Toledo, Greifensee, Switzerland). The mediolateral radiographs of bones allowed to measure the length, outside diameter of the midshaft and cortical thickness of the tibias and humerus.

2.5. Peripheral quantitative computed tomography (pQCT)

Femurs and tibias of OI and Wt mice were scanned with a pQCT Research SA+ (Stratec, Birkenfeld, Germany). The thickness of the slice was 150 µm and the voxel size was 0.07 mm. The thresholds for cortical and trabecular bone were 570 mg/cm^3 and 280 mg/cm^3, respectively. Three transverse slices of each bone were analyzed with the XCT540 software of the pQCT to obtain the internal and external diameters of the cortical bone, the BMD, as well as the polar stress-strain index (SSI), an indirect measure of torsional bone strength. The reproducibility (CV) of the measurements was 2–3% for trabecular BMD and 0.5–1% for cortical BMD.

2.6. MicroComputed tomography (microCT)

Immediately after death, the tibias were removed and stored in saline at −20 °C. Subsequently, they were thawed at 7 °C for 12 h and scanned with a high-resolution microCT system (microCT 40; Scanco Medical AG, Bassersdorf, Switzerland) [43]. The voxel size was 20 µm. The scans (47 slices) were 0.564 mm from the middle of the tibia, in the area explored during the biomechanical three-point bending test. From the binarized images, we evaluated the relative bone volume (BV/TV) and the cortical thickness. The CV of repeated measurements is < 2%.

2.7. Bone biomechanical properties

We thawed frozen tibias at 7 °C overnight and then at room temperature before extracting the fibula. The samples were immersed in physiological saline solution during the different preparation steps.

The tibias were tested up to the 3-point bending fracture using the Instron 1114 servo-control electromechanical system (Instron Corp., High Wycombe, United Kingdom) and applying the load of the actuator in the center of the shaft at a speed of 2 mm/min. The span of the lower support was 6 mm [44]. A customized program analyzed the force-deflection curves and provided the bending stiffness, the slope (S, N/mm) of the linear elastic deformation, the yield load (YL, N), at the boundary between the elastic deformation and plastic deformation, and the ultimate load (UL, N), which is the maximum sustained force at the point of fracture. The Elastic Energy (EE, N.mm) corresponded to the area under the curve to the yield point, and the Plastic Energy (PE, N.mm) to the area under the curve from the yield point to the point of fracture. The reproducibility range of mechanical tests is 3–5%.

2.8. Nanoindentation

The nano-hardness test system NHT (CSM Instruments, Peseux, Switzerland) evaluates the properties of the bone material by recording the force shifts of a pyramidal diamond indenter pressed into the bone [43]. Tibias excised immediately after euthanasia and frozen at −20 °C were thawed at 7 °C overnight. Then they were rehydrated in saline for 16 h. They were cut in the middle of the shaft to perform the indentation in a transverse plane. The mechanical tests included five indentation points as described by Ammann et al. [45] and analyzed the Young's modulus (gPa), also known as stiffness, hardness (mPa), defined as the average pressure that the material can resist, and dissipated energy (mN * nm), calculated from the area under the indentation curve.

2.9. Dynamic histomorphometry

The tibias were included in methyl methacrylate without preliminary decalcification and were cut into 150-µm-thick cross-sections through the midshaft with a rotating diamond saw (Leica SP1600, Nussloch, Germany), as described previously [46]. The sections were sanded manually to obtain a thickness of 100 ± 1 µm. They were then placed on a fine grain holographic emulsion (VRP M, Slavich Geola, Vilnius, Lithuania) and microradiographed with a Machlett tube with anode of tungsten (Baltograph, Balteau, Liège, Belgium). The exposure time was 50′ at 14 kV and 13 mA. The films were revealed with SM-6 developer (Geola), fixed and rinsed in tap water. The microradiographs were photographed under ordinary light microscopy. We acquired fluorescence images of the sections with an Axio Scope.A1 microscope (Zeiss, Jena, Germany, excitation 485/20 nm, emission 540/25 nm). We then delineated the calcein labels in the periosteal and in the endocortical circumference by using the ImageJ program (ImageJ 1.43u, Wayne Rasband, National Institutes of Health, USA). However, we could only delineate the first (day 1) and the last (day 63) labels of calcein because of discontinuity in the intermediate ones. This allowed us to measure the surface of bone between these calcein labels as an estimate of apposition at periosteal and endocortical circumferences of the entire diaphysis rather than at a specific location. Then, we measured the average thickness of the bone apposition between the labels with a ring model to calculate the mineral apposition rate (MAR) and the bone formation rate (BFR) according to the standard nomenclature [47,48].

2.10. Statistics

We present the results as mean ± SD or SEM. The statistical analysis was performed with Sigma-Plot (Systat Software, Inc. San Jose, CA, USA) or GraphPad Prism version 6.00 (GraphPad Software, La Jolla California, USA). The analysis of variance (one-way ANOVA) was followed by post hoc tests such as the Holm-Sidak method.

3. Results

3.1. Survival

The Wt mice treated with Scl-Ab and Veh. completed the 9-week study safely. Among the 20 OI Veh. mice included in the experiment, 3 died during the first 4 weeks and 2 others during the last 5 weeks. In the OI Scl group, including 20 mice at the beginning of experiment, 2 mice died during the first 4 weeks and 2 mice died during the last 5 weeks of treatment. In half of them, the death occurred during the sedation whereas it was unexplained in the others. There was no difference in mortality rate between Veh. and Scl-Ab-treated animals. Therefore these OI groups consisted of 15 and 16 mice, respectively.

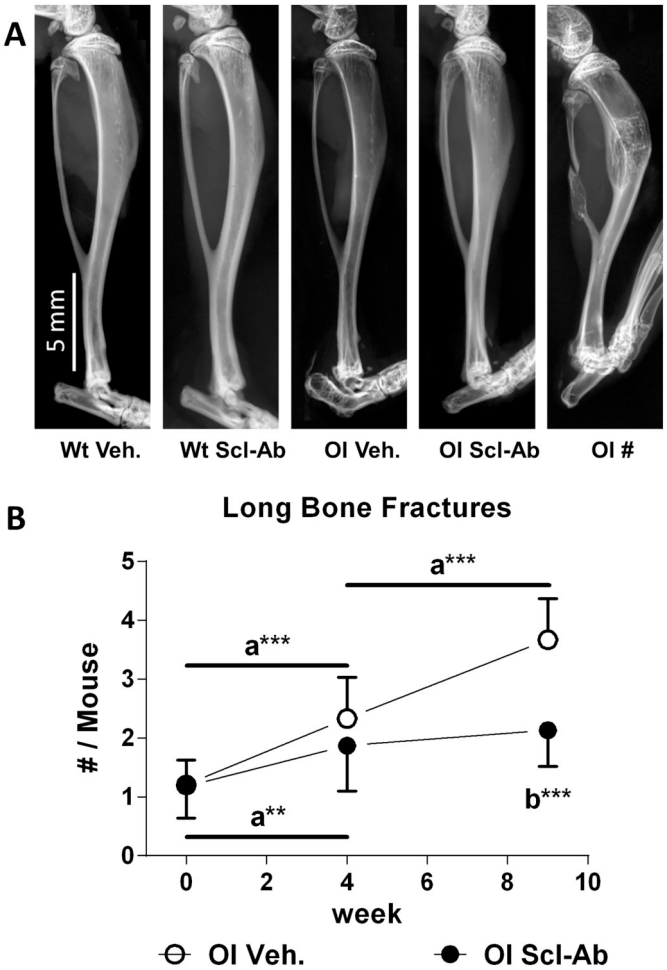

Fig. 1. A: X-rays of one leg (tibia and fibula) of each group. The fracture (OI#) was defined by the evidence of solution of continuity, callus formation, and bone deformity. B: Prevalence of fractures (mean ± SEM) detected with X-rays in all the long bone diaphyses of mice before (week 0) and after treatment with Veh. or with Scl-Ab (weeks 4 and 9). At the beginning of the study, all the mice with OI had long bone fractures, without difference in the average number of fractures between both groups. At the end of the 9-week treatment, the prevalence of diaphyseal bone fractures increased by 205% in the group treated with Veh. and 81% in the group with Scl-Ab. a: baseline (week 0) versus week 4 or week 4 versus week 9 within the same group; b: OI Scl-Ab versus OI Veh; *$p < 0.05$; **$p < 0.01$; ***$p < 0.001$.

3.2. Sclerostin antibody dramatically reduced the incidence of long bone fractures in OI mice

In the radiographic analysis, the radiopacity and cortical thickness of the long bones were lower in the OI treated with Veh. than in Wt mice treated with Veh. Scl-Ab therapy markedly increased radiopacity and cortical thickness of long bones in OI and Wt mice. After a 9-week therapy, radiographs of humerus and tibias appeared similar in OI mice treated with Scl-Ab and Wt mice treated with Veh. (Fig. 1A). Radiographs detected at least one limb fracture in all mice with OI at the start of treatment, but none in the Wt group.

At the beginning of the experiment, the number of fractures per mouse was 1.2 ± 0.8 and 1.18 ± 0.7 in OI mice treated with Vehicle ($n = 10$) and with Scl-Ab ($n = 10$), respectively ($p = 0.820$) (Fig. 1 B). At 4 weeks of the experiment, the same mice from both groups showed a significant increase in the number of fractures, i.e. 2.3 ± 0.7 and 1.8 ± 0.6 per mouse treated with Veh. and Scl-Ab, respectively. From week 4 to 9, OI Veh. had a 57% increase in the prevalence of fractures ($p < 0.001$), while the prevalence of fractures increased by 14% in OI Scl-Ab ($p = 0.709$). At the end of the study, the number of fractures per mouse was significantly lower in OI Scl-Ab than in OI Veh. (2.1 ± 0.8 vs 3.6 ± 0.3, $p < 0.001$; $n = 15$ per group). Thus, from week 1 to week 9, the prevalence of limb fractures increased by 205% in OI Veh. and 81% in OI Scl-Ab. It should be noted that X-rays can detect the anti-fracture effect only after 4 weeks of treatment with Scl-Ab.

In both groups of OI, there was no significant difference in the prevalence of long bone fracture between the forelimb and the hindlimb at 4 weeks of age, before beginning the experiment (data not shown). Scl-Ab therapy markedly reduced the average number of fractures in the different bones, with no difference between the forelimb and the hindlimb.

3.3. Sclerostin antibody decreased bone brittleness

The average stiffness (S) of the tibias, measured by the 3-point bending test, was 67% lower in OI Veh. than in Wt Veh. ($p = 0.01$; Fig. 2A). Scl-Ab significantly increased by 77% and 172% ($p < 0.001$) the mean stiffness of the Wt and OI mice, respectively. At the end of the study, there was no significant difference in tibial stiffness between OI Scl-Ab and Wt Veh. ($p = 0.446$). The ultimate load (UL) of the tibia was significantly lower by 60% in OI Veh. than in Wt Veh. ($p < 0.001$, Fig. 2B). Scl-Ab markedly increased ($p < 0.001$) the mean UL in the tibias of both Wt (+93%) and OI (+86%) mice. At the end of the study, the difference in UL means between OI Scl-Ab and Wt Veh. was at the limit of statistical significance ($p = 0.047$). The yield load (YL) of the tibial shafts of OI Veh. was significantly lower by 63% than that of Wt Veh. tibiae ($p < 0.001$; Fig. 2C). The Scl-Ab therapy increased the mean YL of Wt mice samples by 81% ($p < 0.001$) and by 69% the mean YL of samples from OI mice ($p > 0.05$). However, the mean YL of the OI Scl-Ab samples remained significantly lower than that of the Wt Veh. samples ($p = 0.011$). Plastic energy (PE) was 61% lower in the tibial diaphyses of OI Veh. than in Wt Veh. ($p = 0.049$, Fig. 2D). Scl-Ab therapy significantly improved tibial diaphysis PE in Wt (+61%, $p = 0.03$) and OI mice (+184%, $p = 0.045$). There was no significant difference in tibial PE between OI Scl-Ab and Wt Veh. groups. The average elastic energy (EE) of the tibial shafts of OI Veh. was 27%

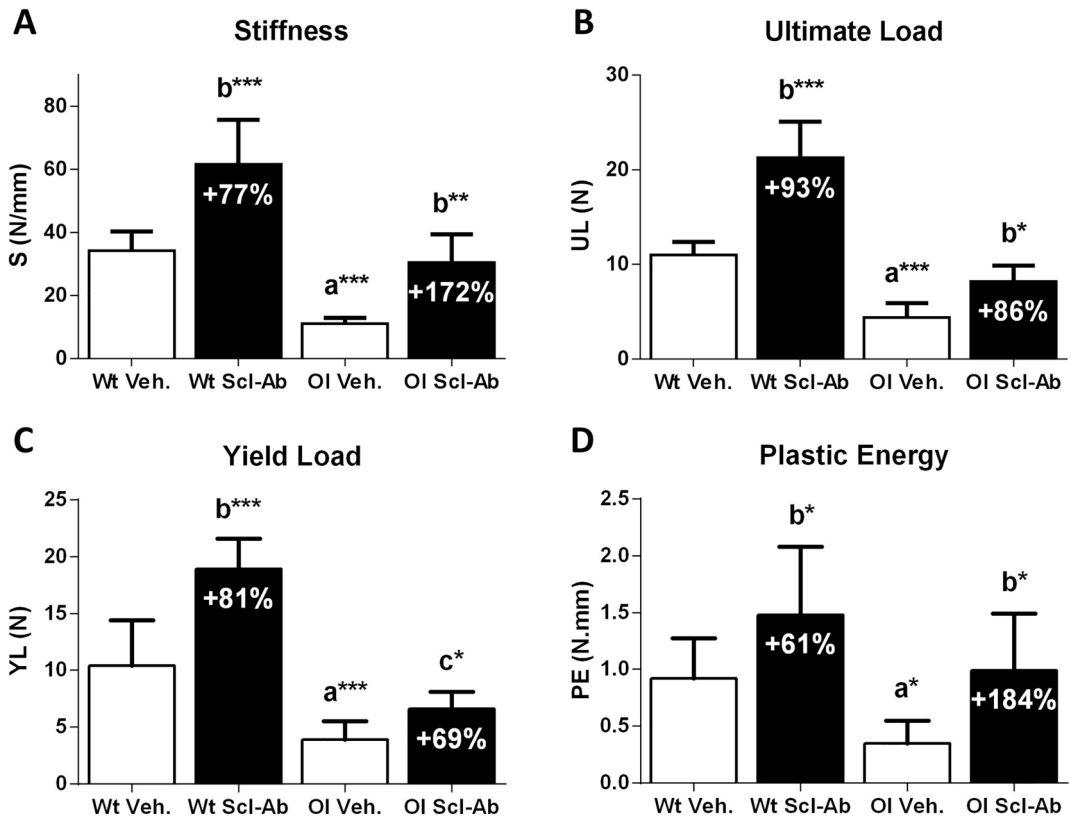

Fig. 2. Data of the test of three-point bending of the tibias after 9 weeks of treatment with antibodies against sclerostin (Scl-Ab) or Vehicle/PBS (Veh.) (mean ± SD). A: the average stiffness (S, N/mm) was 67% lower in the midshaft tibias of the OI Veh. that Wt Veh. The mean stiffness increased significantly in the tibias of the Wt and OI mice after Scl-Ab. B: the average ultimate load (UL, N) of the tibias of OI Veh. was 60% lower than that of the Wt Veh. specimens. Treatment with Scl-Ab significantly increased the ultimate load in both groups. C: The average yield load (YL, N) of OI Veh. tibias was 63% lower than Wt Veh. Scl-Ab significantly improved the mean YL of the tibias in both Wt mice groups. D: The mean plastic energy (PE, N.mm) of the tibias was lower by 62% in OI Veh. than Wt Veh. Scl-Ab significantly increased the mean PE of the tibias of Wt and OI mice. Wt Veh.: $n = 12$; Wt Scl-Ab: $n = 13$; OI Veh.: $n = 8$; OI Scl-Ab: $n = 8$; a: OI Veh. versus Wt Veh.; b: Scl-Ab versus Veh.; c: OI Scl-Ab versus Wt Veh.; * $p < 0.05$; ** $p < 0.01$; *** $p < 0.001$.

Table 1
Bone mineral density (BMD) and polar stress/strain index (SSI) measured by pQCT in femur and tibia midshafts of wildtype (Wt) and oim/oim (OI) mice after 9-week treatment with either Scl-Ab or PBS/Vehicle (Veh.).

	Wt Veh.	Wt Scl-Ab	OI Veh.	OI Scl-Ab
Femur	$n = 27$	$n = 27$	$n = 18$	$n = 15$
BMD (mg/cm^3)	743 ± 60 c**	910 ± 45 b***	542 ± 55 a***	682 ± 75 b***
SSI polar (mm^3)	0.53 ± 0.07	0.89 ± 0.15 b***	0.29 ± 0.02 a***	0.47 ± 0.08 b***
Tibia	$n = 10$	$n = 10$	$n = 10$	$n = 10$
BMD (mg/cm^3)	886 ± 68	1058 ± 56 b***	740 ± 65 a***	950 ± 88 b***
SSI polar (mm^3)	0.24 ± 0.05	0.44 ± 0.09 b***	0.15 ± 0.05 a*	0.24 ± 0.05 b*

Values are mean ± SD; a: OI Veh. versus Wt Veh.; b: Scl-Ab versus Veh.; c: OI Scl-Ab versus Wt Veh.
* $p < 0.05$.
** $p < 0.01$.
*** $p < 0.001$.

inferior to that of the Wt Veh. samples ($p = 0.094$; data not shown). The therapy with Scl-Ab significantly improved the EE of the tibial diaphyses in Wt mice (+109%, $p < 0.001$), but not in OI mice (−14%, $p = 0.570$).

The above results indicate that Scl-Ab therapy drastically reduced the prevalence of limb fractures in OI mice and markedly improved the biomechanical properties of the OI tibias. Therefore, we evaluated the impact of Scl-Ab on several determinants of bone strength, including bone mass, geometry (shape and microarchitecture) and mechanical properties at the tissue level [8].

3.4. Sclerostin-antibody increased BMD of femur and tibia diaphyses

In the absence of Scl-Ab, bone mineral density (BMD), measured with pQCT, was significantly lower by 27% in the femur and 16% in the midshaft of tibia of the OI than Wt mice ($p < 0.001$, Table 1). Scl-Ab therapy significantly improved BMD in both OI (+26% and +28% in the femur and tibia, respectively) and Wt mice (+22% in the femur and +19% in the tibia) ($p < 0.001$). At the end of the study, there were no significant differences in the mean BMD between OI Scl-Ab and Wt Veh. tibia midshafts and between OI Scl-Ab and Wt Veh. femur midshafts ($p > 0.05$).

The polar stress/strain index (SSI) was significantly lower the midshaft of the femur (−45%) and tibia (−38%) of OI Veh. than in the corresponding wildtype samples (Table 1). Scl-Ab therapy significantly improved the mean SSI of the femur and tibia midshafts in OI and Wt animals: +68% in Wt femur, +62% in OI femur, +83% in Wt tibia and +60% in OI tibia. After the 9-week therapy, there was no significant difference in mean SSI between OI Scl-Ab femur and Wt Veh. femur, as well as between OI Scl-Ab tibia and Wt Veh. tibia.

Bone resistance to bending and torsional loads depends not only on the bone mass but also on the distribution of bone mass around the main bending axis [8]. As the changes associated with Scl-Ab were greater in SSI than in BMD, possible modifications in bone geometry were sought after Scl-Ab therapy.

3.5. Sclerostin-antibody improved long bone geometry

In OI Veh., the average length of the humerus and the tibia was significantly less than in Wt Veh. (−4% and −7%, respectively, $p < 0.05$) (Table 2). Scl-Ab therapy did not change the average length of these bones in both groups. The diameter of the midshaft of the humerus and the tibia was also significantly lower in OI mice than in Wt mice (−8% and −11%, respectively). Consistently, the average external volume of OI Veh. tibia was 30% lower than in Wt Veh. tibia. Scl-Ab significantly increased the average diameter of the midshaft of the humerus and the tibia in both Wt and OI mice (+6% and +10% in Wt and OI humerus, respectively; +16% and +14% in Wt and OI tibia, respectively). These changes were associated with a significant increase in the external volume of the tibia, 35% in OI and 21% in Wt ($p < 0.001$). At the end of the therapy, there was no significant difference in the mean diameter of the tibial midshaft between OI Scl-Ab and Wt Veh. and the diameter of the midshaft of the humerus was greater in OI Scl-Ab than in Wt Veh.

The cross sections through the tibial midshaft (Fig. 3) observed with pQCT (A), microCT (B) and microradiography (C) illustrate the positive effect of Scl-Ab on diaphyseal diameter, as well as cortical thickness and the cortical bone area in both OI and Wt mice. The corresponding quantitative data are detailed in Table 3.

In animals treated with Veh., both the mean cortical bone volume (BV) and the total volume (TV) were significantly lower in the OI than in the Wt tibia (−25% and −22%, respectively). The average cortical BV/TV ratio was also significantly lower by 9% in OI than in Wt tibia. After 9 weeks of therapy with Scl, the average BV, TV and BV/TV increased significantly in the Wt and OI tibias. In wildtype samples, BV increased by 65%, TV by 38% and BV/TV by 18%. In the OI samples, the increase was 53% for the average BV, 24% for the average TV and 23% for the average BV/TV. The mean cortical thickness of the

Table 2
Length and midshaft diameter of humerus and tibia measured by X-ray analyses and external volume of tibia assessed by Archimedes' principle in wildtype (Wt) and oim/oim (OI) mice after 9-week treatment with either Scl-Ab or PBS/Vehicle (Veh.).

	Wt Veh.	Wt Scl-Ab	OI Veh.	OI Scl-Ab
Humerus	$n = 12$	$n = 12$	$n = 8$	$n = 12$
Length (mm)	12.2 ± 0.1 c*	12.3 ± 0.1	11.7 ± 0.1 a*	11.8 ± 0.1
Diameter (mm)	1.31 ± 0.01 c***	1.39 ± 0.01 b**	1.21 ± 0.02 a***	1.33 ± 0.02 b***
Tibia	$n = 12$	$n = 12$	$n = 8$	$n = 12$
Length (mm)	17.7 ± 0.1 c**	18.1 ± 0.1	16.4 ± 0.3 a***	16.8 ± 0.2
Diameter (mm)	1.13 ± 0.02	1.31 ± 0.02 b***	1.01 ± 0.02 a**	1.15 ± 0.02 b***
Volume (μl)	0.33 ± 0.01	0.40 ± 0.01 b***	0.23 ± 0.01 a***	0.31 ± 0.01 b***

Values are mean ± SEM; a: OI Veh. versus Wt Veh.; b: Scl-Ab versus Veh.; c: OI Scl-Ab versus Wt Veh.
* $p < 0.05$.
** $p < 0.01$.
*** $p < 0.001$.

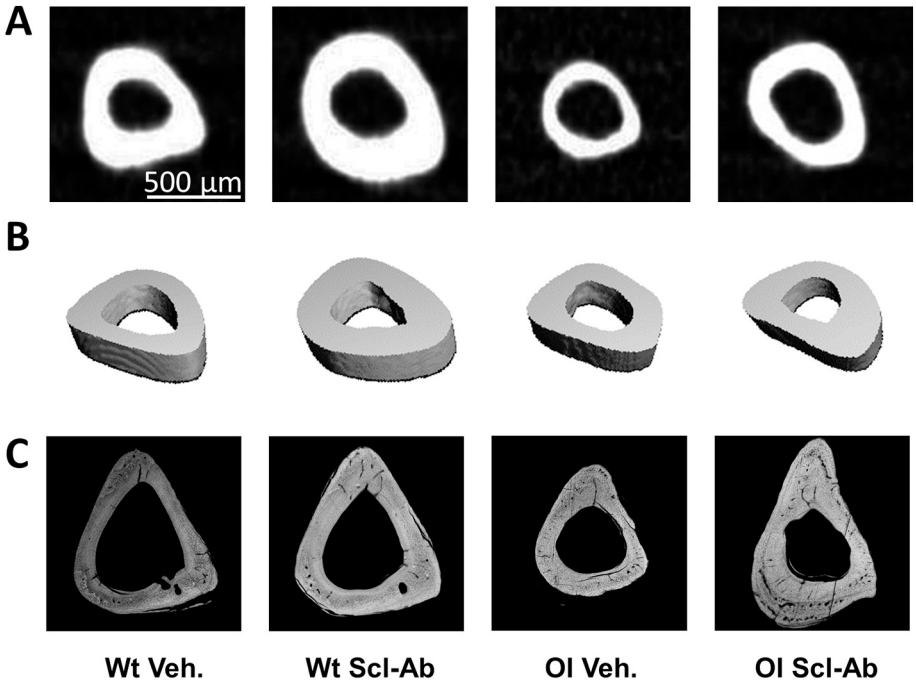

Fig. 3. Transverse sections of midshaft tibias observed with pQCT (A), microCT (B) and microradiography (C) illustrating differences in bone mass and geometry between OI Veh. and Wt Veh. mice, as well as the positive effect of Scl-Ab on these characteristics in both groups.

midshafts of the tibia and femur was 16–17% significantly lower in the OI than in the wildtype samples. Scl-Ab therapy significantly increased the mean cortical thickness of these long bones in Wt and OI mice ($p < 0.001$). This increase in femoral cortical thickness was 35% in Wt mice and 27% in OI mice. The increase in tibial cortical thickness was 48% in Wt mice and 42% in OI mice.

Microradiographs of OI tibial sections also showed abundant vascular channels, particularly at the periosteal surfaces of Scl-Ab treated mice, corresponding to the location of calcein labels (Fig. 4A). Furthermore, at higher magnification, they highlighted more numerous osteocyte lacunae in OI than WT bone tissue (not illustrated).

Fluorescence microscopy highlighted more extensive calcein labels on the endocortical and periosteal surfaces of the tibias after Scl-Ab therapy than after vehicle treatment (Fig. 4A). The distances between successive labels, corresponding to the amount of bone deposited during the time interval, also appeared higher in OI Scl-Ab than in OI Veh. on both endocortical and periosteal surfaces. As we did not observe any difference in the mineral apposition rate (MAR) between successive labels, we considered the thickness of the bone between the first and the last label. The periosteal MAR was 38% lower and the average bone formation rate/bone surface (BFR/BS) by 18% in the tibia of OI Veh. than in Wt Veh. animals ($p > 0.05$) (Fig. 4B-C). The treatment of OI mice with Scl-Ab increased the MAR (+128%; $p < 0.001$) and, consistently, BFR/BS by 78% ($p < 0.01$). At the end of therapy, BFR/BS was significantly higher in OI Scl-Ab than in Wt Veh. ($p < 0.05$). In vehicle-treated animals, the mean endocortical MAR of OI mice was significantly lower by 40% ($p < 0.05$) than in Wt mice (Fig. 4D-E). There was also a 13% reduction in the mean BFR/BS of OI mice, but the decrease in BFR/BS was not statistically significant. Scl-Ab therapy significantly increased the average endocortical MAR in OI mice by 90% ($p < 0.001$). However, this significant increase was not associated with a significant improvement in mean BFR/BS, as observed in the periosteal surface. In Wt mice, Scl-Ab increased mean MAR by 28% and mean BFR/BV by 12%, but these changes did not reach statistical significance.

The above data demonstrated that Scl-Ab therapy markedly improved the geometry of the long bones OI and Wt. Considering the intrinsic properties of the bone matrix are another crucial determinant of bone strength, we investigated the effect of Scl-Ab therapy on the tissue-level mechanical properties of the cortical bone of OI and Wt mice.

Table 3
Midshaft cross-sectional Bone Volume (BV), Total Volume (TV), Bone Volume/Total Volume (BV/TV) and Cortical Thickness (CT) of tibia and Cortical Thickness of femur assessed by microCT in wildtype (Wt) and oim/oim (OI) mice after 9-week treatment with either Scl-Ab or PBS/Vehicle (Veh.).

	Wt Veh.	Wt Scl-Ab	OI Veh.	OI Scl-Ab
Tibia	$n = 12$	$n = 12$	$n = 8$	$n = 8$
BV (mm^3)	0.20 ± 0.03	0.33 ± 0.03 b***	0.15 ± 0.02 a**	0.23 ± 0.02 b***
TV (mm^3)	0.32 ± 0.03	0.44 ± 0.03 b***	0.25 ± 0.02 a***	0.31 ± 0.02 b**
BV/TV (%)	64.0 ± 3.1 c***	75.3 ± 2.4 b***	58.6 ± 4.8 a**	72.1 ± 1.7 b***
CT (mm)	0.23 ± 0.03 c*	0.34 ± 0.03 b***	0.19 ± 0.02 a*	0.27 ± 0.02 b***
Femur	$n = 13$	$n = 16$	$n = 12$	$n = 11$
CT (mm)	0.31 ± 0.03	0.42 ± 0.05 b***	0.26 ± 0.03 a*	0.33 ± 0.04 b***

Values are mean ± SD; a: OI Veh. versus Wt Veh.; b: Scl-Ab versus Veh.; c: OI Scl-Ab versus Wt Veh.
* $p < 0.05$.
** $p < 0.01$.
*** $p < 0.001$.

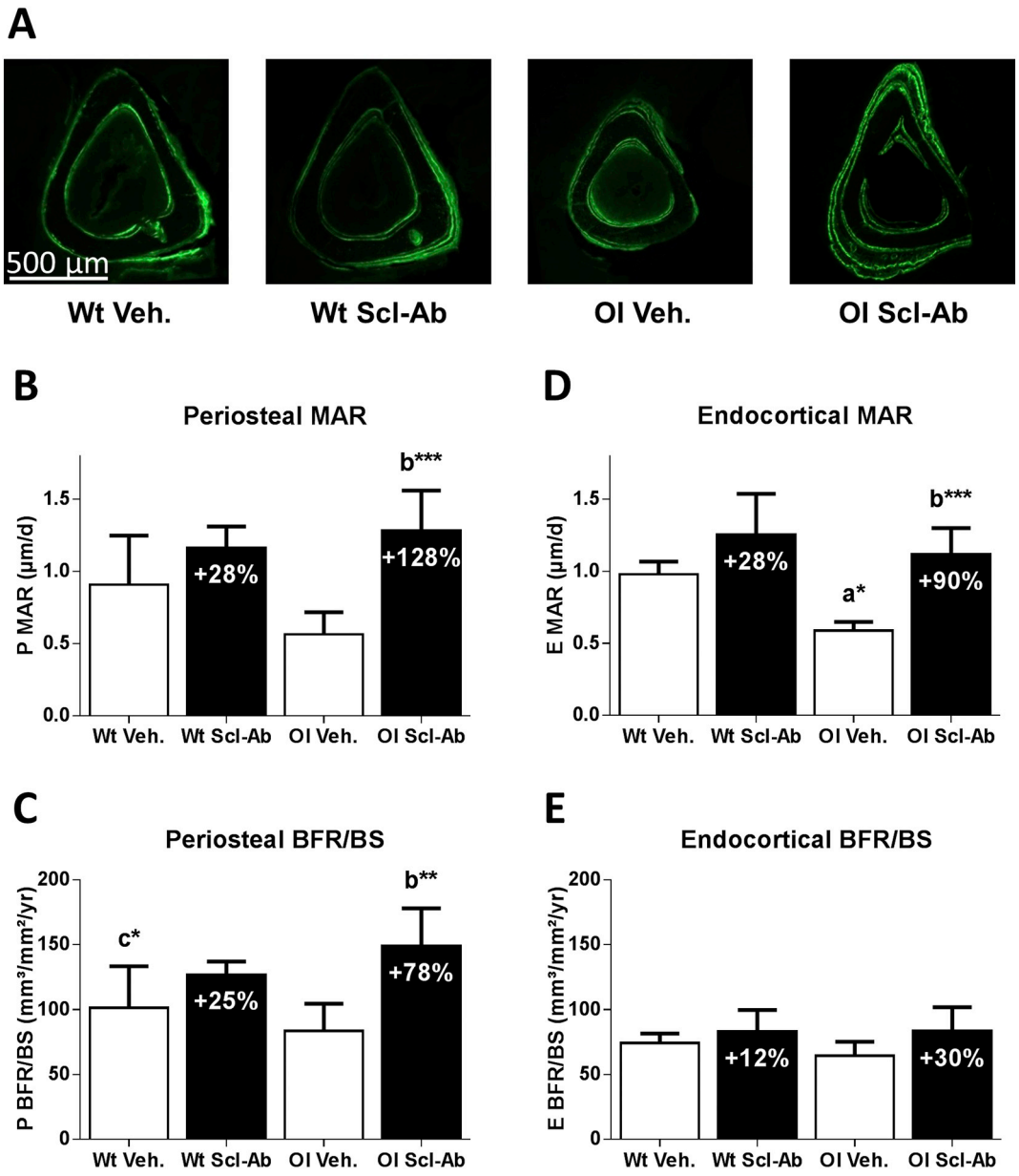

Fig. 4. Dynamic histomorphometry in the tibial midshaft. A: Fluorescence microscopy appearance of a cross section through the tibial mid-diaphysis of OI and Wt mice treated with Scl-Ab or with Veh. and showing calcein green labels on periosteal and endocortical surfaces. The calcein was injected on days 1, 21, 42 and 63. B. Periosteal mineral apposition rate (MAR). MAR was lower in OI Veh. than Wt Veh. tibia and increased significantly in OI mice after treatment with Scl-Ab. C. The periosteal bone formation rate/bone surface rate (BFR/BS) increased in OI mice after treatment and was significantly higher in OI Scl-Ab than in Wt Veh. Increases in MAR and BFR/BS in Wt mice did not reach statistical significance. D. In animals treated with vehicle, the endocortical MAR was significantly lower in OI mice compared to Wt mice. Scl-Ab therapy strongly improved the MAR mean in OI mice but not in Wt mice. E. Scl-Ab did not have a significant effect on endocortical BFR/BS in OI mice and Wt mice. Data are expressed as mean ± SD. Wt Veh.: $n = 5$; Wt Scl-Ab: $n = 5$; OI Veh.: $n = 5$; OI Scl-Ab: $n = 6$; a: OI Veh. versus Wt Veh.; b: Scl-Ab versus Veh.; c: OI Scl-Ab versus Wt Veh.; *$p < 0.05$; **$p < 0.01$; ***$p < 0.001$. (For interpretation of the references to colour in this figure legend, the reader is referred to the web version of this article.)

3.6. Sclerostin-antibody did not change tissue intrinsic properties of OI long bones

In the animals treated with Veh., we did not observe significant difference in the mean Young's modulus of the cortical bone between the OI and the Wt, as measured by nanoindentation (Table 4). In contrast, in the OI bone samples, the mean hardness of the tissue and the dissipated energy were significantly higher by 32% and 16%, respectively, than in the wildtype samples. In Wt mice, Scl-Ab significantly increased the mean Young's modulus by 6% ($p < 0.01$), the average tissue hardness by 13% ($p < 0.05$) and the mean dissipated energy by 12% ($p < 0.001$). Treatment of OI mice with Scl-Ab did not significantly increase this nanoindentation data (average increase < 4%).

4. Discussion

Consistent with the main phenotypic characteristics of osteogenesis imperfecta (OI) type III in humans, i.e., skeletal fragility with numerous fractures and bone deformability, oim/oim mice (OI mice) presented spontaneous long bone fractures [39] associated with weak mechanical resistance, low bone mass, and poor bone quality. Our data showed that the treatment with the antibody against sclerostin (Scl-Ab) improves the mechanical properties of the long bones of OI mice while increasing

Table 4
Nanoindentation mechanical properties (Young's modulus, hardness and dissipated energy) of midshaft tibia from wildtype (Wt) and oim/oim mice after 9-week treatment with either Scl-Ab or PBS/Vehicle (Veh.).

	Wt Veh.	Wt Scl-Ab	OI Veh.	OI Scl-Ab
Nanoindentation	$n = 12$	$n = 13$	$n = 10$	$n = 8$
Modulus (gPa)	18.2 ± 0. 2 c**	19.3 ± 0.2 b**	18.5 ± 0.2	19.3 ± 0.3
Hardness (mPa)	558 ± 13 c***	629 ± 13 b*	735 ± 22 a***	760 ± 20
Dissipated energy (mN*nm)	3715 ± 59 c***	4172 ± 81 b***	4319 ± 85 a***	4489 ± 83

Values are mean ± SEM; a: OI Veh. versus Wt Veh.; b: Scl-Ab versus Veh.; c: OI Scl-Ab versus Wt Veh.
* $p < 0.05$.
** $p < 0.01$.
*** $p < 0.001$.

the osteoblastic apposition, the bone mineral density (BMD) and the microCT morphometric characteristics of the cortical bone. These changes were associated with a significant reduction in the number of long bone fractures in mice with OI.

The oim/oim mouse is one of the most appropriate animal models of human OI type III [39,40]. In contrast to other studies (Table 5), we used only female mice because they are known to be more fragile and to have lower bone mass and bone bending and torsional strength than their male counterparts [49]. Moreover, the external diameter of long bones is smaller in female than in male mice from 4 to 40 weeks of age [50]. By focusing on females, we did not obtain comparative data from male OI mice. However, such a comparison should be considered in order to highlight gender-related differences in phenotype severity and in response to Scl-Ab.

Currently, bisphosphonates (BP) are the most common treatment for patients with OI. As explained above, they improve the density and geometry of trabecular and cortical bone. However, BP have side effects, such as esophageal irritation and, when administered intravenously, acute phase response [23,51]. In addition, their efficacy in decreasing the rate of long bone fractures is not clearly established [16,18]. In fact, in several murine models of moderate to severe forms of OI, the BP mainly increased the trabecular bone and, despite improved cortical bone mass, they did not seem to increase the in vivo strength of long bone [52,53]. The denosumab RANKL-antibody, a reversible antiresorptive compound, also failed to reduce the fracture rate of long bones in the oim/oim mouse model of severe OI [54]. In children with OI (type I, III and IV), denosumab lead to inconsistent effects on fracture rates, although BMD in the lumbar region was significantly improved [55]. In children with type I and IV OI (mild and moderate, respectively), GH increases the rate of growth and bone mineral density (BMD) but does not change the risk of fracture. In addition, GH has no beneficial effect in patients with type III OI [56]. Teriparatide (PTH 1–34) has an anabolic effect in postmenopausal osteoporosis [57–59], but the compound cannot be prescribed to children because young rats treated with PTH develop osteosarcoma [60].

This disappointing effectiveness of BP and other treatments led to investigate new therapeutic approaches. Romosozumab, a sclerostin antibody (Scl-Ab), improved BMD of the lumbar spine, total hip and femoral neck in postmenopausal women with low bone mineral density [61]. Romozumab exerts a double effect on bone, with a transient increase in markers of bone formation (P1NP serum, bone-specific alkaline phosphatase, osteocalcin) and, conversely, reduction in markers of bone resorption (serum β-CTX) [31,62]. Similar effects have also been observed in animal models of osteoporosis [63,64]. Recently, we demonstrated that treatment with Scl-Ab increased the trabecular BMD, connectivity, and resistance to the compressive force of the vertebrae of OI mice while decreasing the fracture rate of the pelvis and tail vertebrae [65].

To our knowledge, the data relative to the number of axial and appendicular fractures in patients with OI are infrequent and incomplete, with some studies reporting the clinical characteristics and the fracture pattern at the time of diagnosis, without any lifetime evaluation [66,67]. The authors who used oim/oim mice generally considered the axial and appendicular fractures indistinctly (Table 5). Only two articles focused only on long bones of OI mice [68,69]. For this reason, the present study specifically analyzes long bone. Indeed, we observed 2.9 ± 0.3 spontaneous fractures in the tail and pelvis per mouse with OI after 9 weeks of Veh. treatment [65], which was less than in long bones (Fig. 1B). This difference attests to the relevance of considering axial and long bone data separately, as representative of trabecular and cortical bone, respectively. This distinction allowed to support the hypothesis of a specific effect of the treatment on the fracture rate after 9 weeks of treatment, since OI Scl-Ab suffered 1.1 ± 0.2 axial [65] and 2.1 ± 0.8 appendicular fractures per mouse. The number of long bone fractures at the beginning of the experiment was slightly less than the number reported by Bargman et al. (2010) at 6 weeks of age (Table 5). These data are consistent with those observed in studies that group axial and appendicular bone fractures [52,53,70].

As observed with X-rays, therapy with Scl-Ab should last more than a month, since we did not detect any difference in the long bone fracture rate between both OI groups after 4 weeks of the experiment. After 9 weeks of treatment, the prevalence of diaphyseal fractures in the Scl-Ab group had increased to a significantly lesser extent than in the vehicle group. Until now, except similar data observed in OI femur after

Table 5
Fracture incidence reported in oim/oim mice according to gender, age, treatment and bones analyzed.

Reference	Gender	Age	Treatment	Treatment duration	Bones	Number of fractures/mouse (SD)		
						Initial	Vehicle	Treatment
Camacho et al. 2001 [52]	M&F	6 weeks	ALN	8 weeks	humerus, femur, tibia, tail	1.5	3.2 (1.6)	2.1 (2)
McCarthy et al. 2002 [53]	M&F	2 weeks	ALN	14 weeks	humerus, femur, tibia, tail	0.7 (0.8)	2 (0.2)	0.7 (0.7)
Bargman et al. 2010 [68]	M&F	6 weeks	RANK-Fc	8 weeks	humerus, femur, tibia	1.8	2.5 (1.4)	2.47 (0.9)
Bargman et al. 2012 [54]	M&F	2 weeks	RANK-Fc/ALN	12 weeks	humerus, radius, femur, tibia, tail	/	9 (3)	4.3 (3)/4.4 (2.7)
Boskey et al. 2015 [83]	M	2 weeks	RANK-Fc	12 weeks	axial and appendicular	/	4 (2)	/
Boskey et al. 2015 [83]	F	2 weeks	RANK-Fc	12 weeks	axial and appendicular	/	2 (2)	/
Berman et al. 2016 [69]	M	8 weeks	RAL	8 weeks	femur	/	48% (13/27)	20% (6/30)
Shi et al. 2016 [70]	F	3 weeks	SrR	11 weeks	humerus, radius, femur, tibia, tail	1.2 (0.8)	3.7 (1.1)	1.9 (1.3)

ALN: alendronate; RANK-Fc: Receptor activator of nuclear factor kappa B ligand inhibition; RAL: raloxifène; SrR: strontium ranelate.

treatment with raloxifene [69], no other study demonstrated such a specific decrease in the occurrence of long bone fractures (Table 5).

Other treatments, such as alendronate [52,53], RANKL [59], raloxifene [69] and strontium ranelate [70], were shown to increase bone strength in mice with OI. Some of these studies [52,53,69,70] also reported less numerous fractures in treated than untreated mice (Table 5). In one of them, alendronate was administered from 2 weeks of age to influence total growth; the number of fractures remained unchanged after 14 weeks [53]. The fractures could have been less numerous in OI Scl-Ab if we had started the treatment 2 or 3 weeks earlier. Furthermore, without similar data in male counterparts, we can only hypothesize some gender-related differences. Indeed, a former study showed that the fracture rate was higher in OI women than in OI men in childhood, in adolescence and even more during the menopause [7]. At the end of adolescence, OI girls seem to have a higher bone mineral density than OI boys [71]. However, in adult humans with OI (age 44 ± 12 years), others have observed more frequent fractures in men than women [5].

Due to a poor periosteal bone formation, the external diameter of the long bones and their cortical thickness are smaller in OI patients than in the normal subjects [26]. These changes in the geometry of the diaphysis were observed in Veh. OI mice, like in Brtl/+ [32,33], in col1a2$^{+/p.G610C}$ [36,37], in Col1a1^{Jrt}/+ [34] and in Crtap−/− [35], and they significantly reduce the resistance of the bone to bending and torsion, which is the main cause of fracture. Consistent with a lower occurrence of fractures, Scl-Ab treatment improved the biomechanical properties of the OI mice bones and increased their bone mass parameters to such a point that they were almost similar to those of Wt Veh. As detailed in the methods, biomechanical tests and morphometry were performed only on intact bones, devoid of any deformation or fracture. Besides the variability related to the site of fracture and the healing phase, the data of OI bones could have been somewhat different if we had measured fractured bones. Nevertheless, in growing Col1a1^{Jrt}/+ mice, another severe dominant OI model, Scl-Ab treatment did not improve biomechanical resistance of the femur, despite an increase in the cortical thickness [34]. In Crtap −/− and in Brtl/+, Scl-Ab increased the biomechanical strength of the femur as well as its cross-sectional bone volume and cortical thickness [35,72]. Similar results were obtained by LRP5 deletion in col1a2$^{+/p.G610C}$ mice [37]. All these studies analyzed cortical bone mass and strength at the end of 4 [34], 5 [72] and 6 [35] weeks of antisclerostin treatment. However, no data are available about such effects several days or weeks later. This point deserves to be investigated in order to determine the total duration of the therapeutic effect.

Scl-Ab has a primary impact on osteoblastic activity [73], but it also negatively regulates osteoclast activity [74,75]. The dynamic histomorphometry data of the tibial cortical bone showed a lower bone formation activity in OI than in Wt mice but this difference was not significant. However, Scl-Ab significantly improved periosteal and endocortical apposition in OI mice tibia. This contributed to enhance its polar SSI, attesting a better distribution of cortical bone from the center of gravity. This parameter is a crucial factor of the resistance of long bones while their matrix composition remained unchanged.

In this study, the hardness and dissipated energy of the bone matrix were higher in OI mice than in Wt mice. In the OI patients, deficient type I collagen molecules provide an abnormal scaffold for the deposition of minerals, decrease bone plasticity and favor the formation of microcracks. Furthermore, the greater extension of the vascular channels supports the growth of failure [76]. Indeed, oim/oim bones were shown to have more numerous vascular channels and osteocyte lacunae than WT, without impacting total cortical porosity, but increasing the risk of failure, as demonstrated with synchrotron tomography and microarchitectural finite elements [77].

The quality of the bone matrix was not modified, whatever the treatment tested, antisclerostin antibody [78], bisphosphonate [24,52,53], RANKL inhibitor [68] or raloxifene [69]. These molecules do not interfere with the composition of the matrix. Scl-Ab treatment induced changes in the nanoindentation data in Wt mice but not in OI mice, as also reported in Brtl/+ mice [32]. Previous observations in the trabecular bone of Col1a1frt/+ mice led to the hypothesis that a substantial proportion of type I procollagen secreted by osteoblasts was not integrated into the bone matrix, whereas the PINP marker increased in serum [34]. Given that the oim phenotype results from a null mutation in exon 52 of the Col1a2 gene [41], homozygous oim/oim mice do not express the col1α2 protein and produce homotrimeric col1α1 instead of the heterotrimer assembled from two α1 chains and an α2 chain. As in Col1a1frt/+ mice, abnormal homotrimeric collagen could be incompletely incorporated into the bone matrix of OI mice, which explains a lower cortical BFR [79]. Additional research should be conducted to understand the difference in the effectiveness of Scl-Ab treatment in the bone matrix of Wt and OI mice. Furthermore, since Sost KO mice did not show any change in lacunar or vascular porosity in tibia cortical bone as compared with WT counterparts [29], we can hypothesize that Scl-Ab did not modify the number of vascular channels, which was visible in the low-resolution microradiography of Scl-Ab tibia.

Although sclerostin deficiency in Van Buchem disease leads to high stature [80], tibias and humerus of Scl-Ab OI mice remained shorter than those of Wt mice. In a previous study [65], we showed that OI mice were smaller than Wt mice and that Scl-Ab did not change this difference in stature. Consequently, the short stature phenotype of the OI mice affects both the axial and the appendicular skeleton. In Sost deficient mice, the length of the tibia is not different from WT mice [29]. Scl-Ab treatment was reported to have no effect on the femur and tibia length of Brtl/+ mice [32,72]. Furthermore, Camacho et al. demonstrated that alendronate, a third-generation bisphosphonate therapy, reduced femur length in 6-week-old mice with OI [52,81]. This important point should be taken into account in the possible treatment of young patients with OI.

The mortality of our OI mice litters corresponds to the observations of Shi et al. who treated oim/oim mice with strontium ranelate during 11 weeks [70]. Yao et al. and Chipman et al. [39,49] also reported a lower pup survival but did not quantify it. Earlier, the one-year survival rate of oim/oim mice had been estimated at 50% [24]. To our knowledge, no survival data exist for other strains of mice with severe OI phenotype. Their high mortality rate could result not only from the reduced biomechanical strength of bones and muscles but also from the abnormal aortic wall and cardiac muscle [40,82]. However, although Scl-Ab has been associated with cardiovascular side effects in human [61], our results do not demonstrate that it worsened the low survival rate of oim/oim mice during the experimental time. It would be useful to analyze this parameter with longer treatment or some time after the arrest of treatment.

In conclusion, the treatment with antibody against sclerostin improved the mechanical resistance of the long bones of OI mice while increasing osteoblastic apposition, bone mineral density, and cortical bone geometry. These changes were associated with a significant reduction in the number of long bone fractures. These therapeutic effects may be beneficial to patients suffering from severe forms of osteogenesis imperfecta, with long and unstable bone fractures.

Acknowledgments

The authors thank the Amgen-UCB consortium for providing the anti-sclerostin antibody (DHM). They are grateful to Isabelle Badoud, Jennifer Siebenaler and Walter Hudders for their expertise and assistance.

Fundings

This research is supported by the Medical Scientific Research Fund (FRSM-IREC88A6, DHM) and by the French-speaking Belgian

Association of the Osteogenesis Imperfecta (www.fetealavie.be/, www.afboi.be/).

Conflict of interests

MS Ominsky is a former employee of Amgen. The authors declare that they have no other conflict of interest.

References

[1] D.A. Stevenson, J.C. Carey, J.L. Byrne, S. Srisukhumbowornchai, M.L. Feldkamp, Analysis of skeletal dysplasias in the Utah population, Am. J. Med. Genet. A 158A (5) (2012) 1046–1054.
[2] A. Forlino, W.A. Cabral, A.M. Barnes, J.C. Marini, New perspectives on osteogenesis imperfecta, Nat. Rev. Endocrinol. 7 (9) (2011) 540–557.
[3] F. Rauch, F.H. Glorieux, Osteogenesis imperfecta, Lancet 363 (9418) (2004) 1377–1385.
[4] F.S. Van Dijk, D.O. Sillence, Osteogenesis imperfecta: clinical diagnosis, nomenclature and severity assessment, Am. J. Med. Genet. A 164A (6) (2014) 1470–1481.
[5] L.L. Wekre, E.F. Eriksen, J.A. Falch, Bone mass, bone markers and prevalence of fractures in adults with osteogenesis imperfecta, Arch. Osteoporos. 6 (2011) 31–38.
[6] I.M. Ben Amor, P. Roughley, F.H. Glorieux, F. Rauch, Skeletal clinical characteristics of osteogenesis imperfecta caused by haploinsufficiency mutations in COL1A1, J. Bone Miner. Res. 28 (9) (2013) 2001–2007.
[7] C.R. Paterson, S. McAllion, J.L. Stellman, Osteogenesis imperfecta after the menopause, N. Engl. J. Med. 310 (26) (1984) 1694–1696.
[8] A. Carriero, E.A. Zimmermann, A. Paluszny, S.Y. Tang, H. Bale, B. Busse, T. Alliston, G. Kazakia, R.O. Ritchie, S.J. Shefelbine, How tough is brittle bone? Investigating osteogenesis imperfecta in mouse bone, J. Bone Miner. Res. 29 (6) (2014) 1392–1401.
[9] M.L. Bouxsein, S.K. Boyd, B.A. Christiansen, R.E. Guldberg, K.J. Jepsen, R. Muller, Guidelines for assessment of bone microstructure in rodents using micro-computed tomography, J. Bone Miner. Res. 25 (7) (2010) 1468–1486.
[10] R.H. Engelbert, Y. van der Graaf, R. van Empelen, F.A. Beemer, P.J. Helders, Osteogenesis imperfecta in childhood: impairment and disability, Pediatrics 99 (2) (1997) E3.
[11] R.H. Engelbert, C.S. Uiterwaal, W.J. Gerver, J.J. van der Net, H.E. Pruijs, P.J. Helders, Osteogenesis imperfecta in childhood: impairment and disability. A prospective study with 4-year follow-up, Arch. Phys. Med. Rehabil. 85 (5) (2004) 772–778.
[12] L.H. Gerber, H. Binder, R. Berry, K.L. Siegel, H. Kim, J. Weintrob, Y.J. Lee, S. Mizell, J. Marini, Effects of withdrawal of bracing in matched pairs of children with osteogenesis imperfecta, Arch. Phys. Med. Rehabil. 79 (1) (1998) 46–51.
[13] J.M. Wilkinson, B.W. Scott, A.M. Clarke, M.J. Bell, Surgical stabilisation of the lower limb in osteogenesis imperfecta using the Sheffield telescopic intramedullary rod system, J. Bone Joint Surg. Br. 80 (6) (1998) 999–1004.
[14] T.J. Cho, J.B. Kim, J.W. Lee, K. Lee, M.S. Park, W.J. Yoo, C.Y. Chung, I.H. Choi, Fracture in long bones stabilised by telescopic intramedullary rods in patients with osteogenesis imperfecta, J. Bone Joint Surg. Br. 93 (5) (2011) 634–638.
[15] L.K. Bachrach, L.M. Ward, Clinical review 1: bisphosphonate use in childhood osteoporosis, J. Clin. Endocrinol. Metab. 94 (2) (2009) 400–409.
[16] A.D. Letocha, H.L. Cintas, J.F. Troendle, J.C. Reynolds, C.E. Cann, E.J. Chernoff, S.C. Hill, L.H. Gerber, J.C. Marini, Controlled trial of pamidronate in children with types III and IV osteogenesis imperfecta confirms vertebral gains but not short-term functional improvement, J. Bone Miner. Res. 20 (6) (2005) 977–986.
[17] H. Castillo, L. Samson-Fang, P. American Academy for Cerebral, P. Developmental Medicine Treatment Outcomes Committee Review, Effects of bisphosphonates in children with osteogenesis imperfecta: an AACPDM systematic review, Dev. Med. Child Neurol. 51 (1) (2009) 17–29.
[18] L.M. Ward, F. Rauch, M.P. Whyte, J. D'Astous, P.E. Gates, D. Grogan, E.L. Lester, R.E. McCall, T.A. Pressly, J.O. Sanders, P.A. Smith, R.D. Steiner, E. Sullivan, G. Tyerman, D.L. Smith-Wright, N. Verbruggen, N. Heyden, A. Lombardi, F.H. Glorieux, Alendronate for the treatment of pediatric osteogenesis imperfecta: a randomized placebo-controlled study, J. Clin. Endocrinol. Metab. 96 (2) (2011) 355–364.
[19] T. Palomo, T. Vilaca, M. Lazaretti-Castro, Osteogenesis imperfecta: diagnosis and treatment, Curr. Opin. Endocrinol. Diabetes Obes. 24 (6) (2017) 381–388.
[20] J.C. Marini, Do bisphosphonates make children's bones better or brittle? N. Engl. J. Med. 349 (5) (2003) 423–426.
[21] C.F. Munns, F. Rauch, L. Zeitlin, F. Fassier, F.H. Glorieux, Delayed osteotomy but not fracture healing in pediatric osteogenesis imperfecta patients receiving pamidronate, J. Bone Miner. Res. 19 (11) (2004) 1779–1786.
[22] J.P. Devogelaer, C. Coppin, Osteogenesis imperfecta: current treatment options and future prospects, Treat. Endocrinol. 5 (4) (2006) 229–242.
[23] M.P. Whyte, W.H. McAlister, D.V. Novack, K.L. Clements, P.L. Schoenecker, D. Wenkert, Bisphosphonate-induced osteopetrosis: novel bone modeling defects, metaphyseal osteopenia, and osteosclerosis fractures after drug exposure ceases, J. Bone Miner. Res. 23 (10) (2008) 1698–1707.
[24] N.P. Camacho, L. Hou, T.R. Toledano, W.A. Ilg, C.F. Brayton, C.L. Raggio, L. Root, A.L. Boskey, The material basis for reduced mechanical properties in oim mice bones, J. Bone Miner. Res. 14 (2) (1999) 264–272.
[25] K.D. Evans, S.T. Lau, A.M. Oberbauer, R.B. Martin, Alendronate affects long bone length and growth plate morphology in the oim mouse model for osteogenesis imperfecta, Bone 32 (3) (2003) 268–274.
[26] F. Rauch, R. Travers, A.M. Parfitt, F.H. Glorieux, Static and dynamic bone histomorphometry in children with osteogenesis imperfecta, Bone 26 (6) (2000) 581–589.
[27] R. Baron, G. Rawadi, Targeting the Wnt/beta-catenin pathway to regulate bone formation in the adult skeleton, Endocrinology 148 (6) (2007) 2635–2643.
[28] S. Khosla, J.J. Westendorf, M.J. Oursler, Building bone to reverse osteoporosis and repair fractures, J. Clin. Invest. 118 (2) (2008) 421–428.
[29] H. Mosey, J.A. Nunez, A. Goring, C.E. Clarkin, K.A. Staines, P.D. Lee, A.A. Pitsillides, B. Javaheri, Sost deficiency does not alter bone's lacunar or vascular porosity in mice, Front. Mater. 4 (2017) 27.
[30] H.Z. Ke, W.G. Richards, X. Li, M.S. Ominsky, Sclerostin and Dickkopf-1 as therapeutic targets in bone diseases, Endocr. Rev. 33 (5) (2012) 747–783.
[31] M.R. McClung, A. Grauer, S. Boonen, M.A. Bolognese, J.P. Brown, A. Diez-Perez, B.L. Langdahl, J.Y. Reginster, J.R. Zanchetta, S.M. Wasserman, L. Katz, J. Maddox, Y.C. Yang, C. Libanati, H.G. Bone, Romosozumab in postmenopausal women with low bone mineral density, N. Engl. J. Med. 370 (5) (2014) 412–420.
[32] B.P. Sinder, M.M. Eddy, M.S. Ominsky, M.S. Caird, J.C. Marini, K.M. Kozloff, Sclerostin antibody improves skeletal parameters in a Brtl/+ mouse model of osteogenesis imperfecta, J. Bone Miner. Res. Off. J. Am. Soc. Bone Miner. Res. 28 (1) (2013) 73–80.
[33] B.P. Sinder, L.E. White, J.D. Salemi, M.S. Ominsky, M.S. Caird, J.C. Marini, K.M. Kozloff, Adult Brtl/+ mouse model of osteogenesis imperfecta demonstrates anabolic response to sclerostin antibody treatment with increased bone mass and strength, Osteoporos. Int. 25 (8) (2014) 2097–2107.
[34] A. Roschger, P. Roschger, P. Keplingter, K. Klaushofer, S. Abdullah, M. Kneissel, F. Rauch, Effect of sclerostin antibody treatment in a mouse model of severe osteogenesis imperfecta, Bone 66 (2014) 182–188.
[35] I. Grafe, S. Alexander, T. Yang, C. Lietman, E.P. Homan, E. Munivez, Y. Chen, M.M. Jiang, T. Bertin, B. Dawson, F. Asuncion, H.Z. Ke, M.S. Ominsky, B. Lee, Sclerostin antibody treatment improves the bone phenotype of Crtap mice, a model of recessive osteogenesis imperfecta, J. Bone Miner. Res. 31 (5) (2015) 1030–1040.
[36] D.G. Little, L. Peacock, K. Mikulec, M. Kneissel, I. Kramer, T.L. Cheng, A. Schindeler, C. Munns, Combination sclerostin antibody and zoledronic acid treatment outperforms either treatment alone in a mouse model of osteogenesis imperfecta, Bone 101 (2017) 96–103.
[37] C.M. Jacobsen, L.A. Barber, U.M. Ayturk, H.J. Roberts, L.E. Deal, M.A. Schwartz, M. Weis, D. Eyre, D. Zurakowski, A.G. Robling, M.L. Warman, Targeting the LRP5 pathway improves bone properties in a mouse model of osteogenesis imperfecta, J. Bone Miner. Res. 29 (10) (2014) 2297–2306.
[38] L.M. Ward, F. Rauch, Oral bisphosphonates for paediatric osteogenesis imperfecta? Lancet 382 (9902) (2013) 1388–1389.
[39] S.D. Chipman, H.O. Sweet, D.J. McBride Jr., M.T. Davisson, S.C. Marks Jr., A.R. Shuldiner, R.J. Wenstrup, D.W. Rowe, J.R. Shapiro, Defective pro alpha 2(I) collagen synthesis in a recessive mutation in mice: a model of human osteogenesis imperfecta, Proc. Natl. Acad. Sci. U. S. A. 90 (5) (1993) 1701–1705.
[40] S.M. Carleton, D.J. McBride, W.L. Carson, C.E. Huntington, K.L. Twenter, K.M. Rolwes, C.T. Winkelmann, J.S. Morris, J.F. Taylor, C.L. Phillips, Role of genetic background in determining phenotypic severity throughout postnatal development and at peak bone mass in Col1a2 deficient mice (oim), Bone 42 (4) (2008) 681–694.
[41] J. Saban, M.A. Zussman, R. Havey, A.G. Patwardhan, G.B. Schneider, D. King, Heterozygous oim mice exhibit a mild form of osteogenesis imperfecta, Bone 19 (6) (1996) 575–579.
[42] N. Cesarovic, F. Nicholls, A. Rettich, P. Kronen, M. Hassig, P. Jirkof, M. Arras, Isoflurane and sevoflurane provide equally effective anaesthesia in laboratory mice, Lab. Anim. 44 (4) (2010) 329–336.
[43] L. Maimoun, T.C. Brennan-Speranza, R. Rizzoli, P. Ammann, Effects of ovariectomy on the changes in microarchitecture and material level properties in response to hind leg disuse in female rats, Bone 51 (3) (2012) 586–591.
[44] P. Ammann, J.P. Bonjour, R. Rizzoli, Essential amino acid supplements increase muscle weight, bone mass and bone strength in adult osteoporotic rats, J. Musculoskelet. Neuronal Interact. 1 (1) (2000) 43–44.
[45] P. Ammann, I. Badoud, S. Barraud, R. Dayer, R. Rizzoli, Strontium ranelate treatment improves trabecular and cortical intrinsic bone tissue quality, a determinant of bone strength, J. Bone Miner. Res. 22 (9) (2007) 1419–1425.
[46] M.A. Cornelis, S. Vandergugten, P. Mahy, H.J. De Clerck, B. Lengele, W. D'Hoore, C. Nyssen-Behets, Orthodontic loading of titanium miniplates in dogs: microradiographic and histological evaluation, Clin. Oral Implants Res. 19 (10) (2008) 1054–1062.
[47] D.W. Dempster, J.E. Compston, M.K. Drezner, F.H. Glorieux, J.A. Kanis, H. Malluche, P.J. Meunier, S.M. Ott, R.R. Recker, A.M. Parfitt, Standardized nomenclature, symbols, and units for bone histomorphometry: a 2012 update of the report of the ASBMR histomorphometry nomenclature committee, J. Bone Miner. Res. 28 (1) (2013) 2–17.
[48] A.M. Parfitt, M.K. Drezner, F.H. Glorieux, J.A. Kanis, H. Malluche, P.J. Meunier, S.M. Ott, R.R. Recker, Bone histomorphometry: standardization of nomenclature, symbols, and units. Report of the ASBMR Histomorphometry nomenclature committee, J. Bone Miner. Res. 2 (6) (1987) 595–610.
[49] X. Yao, S.M. Carleton, A.D. Kettle, J. Melander, C.L. Phillips, Y. Wang, Gender-dependence of bone structure and properties in adult osteogenesis imperfecta murine model, Ann. Biomed. Eng. 41 (6) (2013) 1139–1149.
[50] I.A. Bab, Regulation of skeletal remodeling by the endocannabinoid system, Ann. N. Y. Acad. Sci. 1116 (2007) 414–422.
[51] N.B. Watts, D.L. Diab, Long-term use of bisphosphonates in osteoporosis, J. Clin. Endocrinol. Metab. 95 (4) (2010) 1555–1565.

[52] N.P. Camacho, C.L. Raggio, S.B. Doty, L. Root, V. Zraick, W.A. Ilg, T.R. Toledano, A.L. Boskey, A controlled study of the effects of alendronate in a growing mouse model of osteogenesis imperfecta, Calcif. Tissue Int. 69 (2) (2001) 94–101.
[53] E.A. McCarthy, C.L. Raggio, M.D. Hossack, E.A. Miller, S. Jain, A.L. Boskey, N.P. Camacho, Alendronate treatment for infants with osteogenesis imperfecta: demonstration of efficacy in a mouse model, Pediatr. Res. 52 (5) (2002) 660–670.
[54] R. Bargman, R. Posham, A.L. Boskey, E. DiCarlo, C. Raggio, N. Pleshko, Comparable outcomes in fracture reduction and bone properties with RANKL inhibition and alendronate treatment in a mouse model of osteogenesis imperfecta, Osteoporos. Int. 23 (3) (2012) 1141–1150.
[55] G. Li, Y. Jin, M.A.H. Levine, H. Hoyer-Kuhn, L. Ward, J.D. Adachi, Systematic review of the effect of denosumab on children with osteogenesis imperfecta showed inconsistent findings, Acta Paediatr. 107 (3) (2018) 534–537.
[56] E. Monti, M. Mottes, P. Fraschini, P. Brunelli, A. Forlino, G. Venturi, F. Doro, S. Perlini, P. Cavarzere, F. Antoniazzi, Current and emerging treatments for the management of osteogenesis imperfecta, Ther. Clin. Risk Manag. 6 (2010) 367–381.
[57] R.M. Neer, C.D. Arnaud, J.R. Zanchetta, R. Prince, G.A. Gaich, J.Y. Reginster, A.B. Hodsman, E.F. Eriksen, S. Ish-Shalom, H.K. Genant, O. Wang, B.H. Mitlak, Effect of parathyroid hormone (1-34) on fractures and bone mineral density in postmenopausal women with osteoporosis, N. Engl. J. Med. 344 (19) (2001) 1434–1441.
[58] R. Prince, A. Sipos, A. Hossain, U. Syversen, S. Ish-Shalom, E. Marcinowska, J. Halse, R. Lindsay, G.P. Dalsky, B.H. Mitlak, Sustained nonvertebral fragility fracture risk reduction after discontinuation of teriparatide treatment, J. Bone Miner. Res. 20 (9) (2005) 1507–1513.
[59] T. Nakamura, T. Sugimoto, T. Nakano, H. Kishimoto, M. Ito, M. Fukunaga, H. Hagino, T. Sone, H. Yoshikawa, Y. Nishizawa, T. Fujita, M. Shiraki, Randomized Teriparatide [human parathyroid hormone (PTH) 1-34] once-weekly efficacy research (TOWER) trial for examining the reduction in new vertebral fractures in subjects with primary osteoporosis and high fracture risk, J. Clin. Endocrinol. Metab. 97 (9) (2012) 3097–3106.
[60] A. Watanabe, S. Yoneyama, M. Nakajima, N. Sato, R. Takao-Kawabata, Y. Isogai, A. Sakurai-Tanikawa, K. Higuchi, A. Shimoi, H. Yamatoya, K. Yoshida, T. Kohira, Osteosarcoma in Sprague-Dawley rats after long-term treatment with teriparatide (human parathyroid hormone (1-34)), J. Toxicol. Sci. 37 (3) (2012) 617–629.
[61] F. Cosman, D.B. Crittenden, J.D. Adachi, N. Binkley, E. Czerwinski, S. Ferrari, L.C. Hofbauer, E. Lau, E.M. Lewiecki, A. Miyauchi, C.A. Zerbini, C.E. Milmont, L. Chen, J. Maddox, P.D. Meisner, C. Libanati, A. Grauer, Romosozumab treatment in postmenopausal women with osteoporosis, N. Engl. J. Med. 375 (16) (2016) 1532–1543.
[62] R.R. Recker, C.T. Benson, T. Matsumoto, M.A. Bolognese, D.A. Robins, J. Alam, A.Y. Chiang, L. Hu, J.H. Krege, H. Sowa, B.H. Mitlak, S.L. Myers, A randomized, double-blind phase 2 clinical trial of blosozumab, a sclerostin antibody, in postmenopausal women with low bone mineral density, J. Bone Miner. Res. 30 (2) (2015) 216–224.
[63] X. Li, K.S. Warmington, Q.T. Niu, F.J. Asuncion, M. Barrero, M. Grisanti, D. Dwyer, B. Stouch, T.M. Thway, M. Stolina, M.S. Ominsky, P.J. Kostenuik, W.S. Simonet, C. Paszty, H.Z. Ke, Inhibition of sclerostin by monoclonal antibody increases bone formation, bone mass, and bone strength in aged male rats, J. Bone Miner. Res. 25 (12) (2010) 2647–2656.
[64] M.S. Ominsky, F. Vlasseros, J. Jolette, S.Y. Smith, B. Stouch, G. Doellgast, J. Gong, Y. Gao, J. Cao, K. Graham, B. Tipton, J. Cai, R. Deshpande, L. Zhou, M.D. Hale, D.J. Lightwood, A.J. Henry, A.G. Popplewell, A.R. Moore, M.K. Robinson, D.L. Lacey, W.S. Simonet, C. Paszty, Two doses of sclerostin antibody in cynomolgus monkeys increases bone formation, bone mineral density, and bone strength, J. Bone Miner. Res. 25 (5) (2010) 948–959.
[65] M. Cardinal, A. Dessain, D. Chappard, S. Lafont, T. Roels, M.S. Ominsky, B. Lengelé, C. Nyssen-Behets, D.H. Manicourt, Sclerostin antibody improves vertebrae parameters in murine model of severe osteogenesis imperfecta, WCO-IOF-ESCEO 26 Suppl 1, Oral Presentation of Selected Posters at: World Congress on Osteoporosis, Osteoarthritis and Musculoskeletal Diseases; 2015 Mars 26–29; Milan, Italy; Presentation Number: 642, 2015 Available from:https://www.wco-iof-esceo.org/sites/ecceo15/pdfs/wco15-abstractbook.pdf.
[66] E. Brizola, M.B. Zambrano, B.S. Pinheiro, A.P. Vanz, T.M. Felix, Clinical features and pattern of fractures at the time of diagnosis of osteogenesis imperfecta in children, Rev. Paul. Pediatr. 35 (2) (2017) 171–177.
[67] C.S. Greeley, M. Donaruma-Kwoh, M. Vettimattam, C. Lobo, C. Williard, L. Mazur, Fractures at diagnosis in infants and children with osteogenesis imperfecta, J. Pediatr. Orthop. 33 (1) (2013) 32–36.
[68] R. Bargman, A. Huang, A.L. Boskey, C. Raggio, N. Pleshko, RANKL inhibition improves bone properties in a mouse model of osteogenesis imperfecta, Connect. Tissue Res. 51 (2) (2010) 123–131.
[69] A.G. Berman, J.M. Wallace, Z.R. Bart, M.R. Allen, Raloxifene reduces skeletal fractures in an animal model of osteogenesis imperfecta, Matrix Biol. 52-54 (2016) 19–28.
[70] C. Shi, B. Hu, L. Guo, P. Cao, Y. Tian, J. Ma, Y. Chen, H. Wu, J. Hu, L. Deng, Y. Zhang, W. Yuan, Strontium Ranelate reduces the fracture incidence in a growing mouse model of osteogenesis imperfecta, J. Bone Miner. Res. 31 (5) (2016) 1003–1014.
[71] D.J. Kok, C.S. Uiterwaal, A.J. Van Dongen, P.P. Kramer, H.E. Pruijs, R.H. Engelbert, A.J. Verbout, D.H. Schweitzer, R.J. Sakkers, The interaction between Sillence type and BMD in osteogenesis imperfecta, Calcif. Tissue Int. 73 (5) (2003) 441–445.
[72] B.P. Sinder, J.D. Salemi, M.S. Ominsky, M.S. Caird, J.C. Marini, K.M. Kozloff, Rapidly growing Brtl/+ mouse model of osteogenesis imperfecta improves bone mass and strength with sclerostin antibody treatment, Bone 71 (2015) 115–123.
[73] R. Baron, M. Kneissel, WNT signaling in bone homeostasis and disease: from human mutations to treatments, Nat. Med. 19 (2) (2013) 179–192.
[74] N. Kusu, J. Laurikkala, M. Imanishi, H. Usui, M. Konishi, A. Miyake, I. Thesleff, N. Itoh, Sclerostin is a novel secreted osteoclast-derived bone morphogenetic protein antagonist with unique ligand specificity, J. Biol. Chem. 278 (26) (2003) 24113–24117.
[75] X. Tian, W.S. Jee, X. Li, C. Paszty, H.Z. Ke, Sclerostin antibody increases bone mass by stimulating bone formation and inhibiting bone resorption in a hindlimb-immobilization rat model, Bone 48 (2) (2011) 197–201.
[76] C. Albert, J. Jameson, P. Smith, G. Harris, Reduced diaphyseal strength associated with high intracortical vascular porosity within long bones of children with osteogenesis imperfecta, Bone 66 (2014) 121–130.
[77] A. Carriero, M. Doube, M. Vogt, B. Busse, J. Zustin, A. Levchuk, P. Schneider, R. Muller, S.J. Shefelbine, Altered lacunar and vascular porosity in osteogenesis imperfecta mouse bone as revealed by synchrotron tomography contributes to bone fragility, Bone 61 (2014) 116–124.
[78] B.P. Sinder, W.R. Lloyd, J.D. Salemi, J.C. Marini, M.S. Caird, M.D. Morris, K.M. Kozloff, Effect of anti-sclerostin therapy and osteogenesis imperfecta on tissue-level properties in growing and adult mice while controlling for tissue age, Bone 84 (2016) 222–229.
[79] S.W. Chang, S.J. Shefelbine, M.J. Buehler, Structural and mechanical differences between collagen homo- and heterotrimers: relevance for the molecular origin of brittle bone disease, Biophys. J. 102 (3) (2012) 640–648.
[80] R.L. van Bezooijen, A.L. Bronckers, R.A. Gortzak, P.C. Hogendoorn, L. van der Wee-Pals, W. Balemans, H.J. Oostenbroek, W. Van Hul, H. Hamersma, F.G. Dikkers, N.A. Hamdy, S.E. Papapoulos, C.W. Lowik, Sclerostin in mineralized matrices and van Buchem disease, J. Dent. Res. 88 (6) (2009) 569–574.
[81] T.E. Uveges, K.M. Kozloff, J.M. Ty, F. Ledgard, C.L. Raggio, G. Gronowicz, S.A. Goldstein, J.C. Marini, Alendronate treatment of the brtl osteogenesis imperfecta mouse improves femoral geometry and load response before fracture but decreases predicted material properties and has detrimental effects on osteoblasts and bone formation, J. Bone Miner. Res. 24 (5) (2009) 849–859.
[82] B.A. Gentry, J.A. Ferreira, A.J. McCambridge, M. Brown, C.L. Phillips, Skeletal muscle weakness in osteogenesis imperfecta mice, Matrix Biol. 29 (7) (2010) 638–644.
[83] A.L. Boskey, J. Marino, L. Spevak, N. Pleshko, S. Doty, E.M. Carter, C.L. Raggio, Are changes in composition in response to treatment of a mouse model of osteogenesis imperfecta sex-dependent? Clin. Orthop. Relat. Res. 473 (8) (2015) 2587–2598.